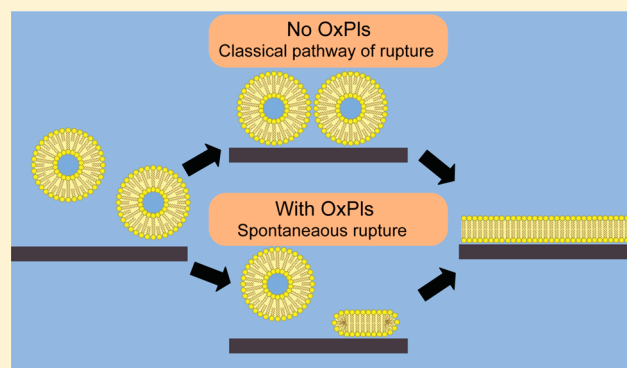


Impact of Lipid Oxidation on Biophysical Properties of Model Cell Membranes

Ali Makky^{†,||} and Motomu Tanaka^{*,†,‡,§}[†]Physical Chemistry of Biosystems, Institute of Physical Chemistry, Heidelberg University, D69120 Heidelberg, Germany[‡]Institute for Toxicology and Genetics, Karlsruhe Institute for Technology, D76021 Karlsruhe, Germany[§]Institute for Integrated Cell-Material Sciences (WPI iCeMS), Kyoto University, 606-8501 Kyoto, Japan

S Supporting Information

ABSTRACT: The oxidation of glycerophospholipids in cell membranes due to aging and environmental stresses may cause a variety of pathological and physiological consequences. A variety of oxidized phospholipid products (OxPL) are produced by the chemical oxidation of unsaturated hydrocarbon chains, which would significantly change the physicochemical properties of cell membranes. In this work, we constructed cell membrane models in the absence and presence of two stable oxidized lipid products and investigated their impact on physical properties of supported membranes using quartz crystal microbalance with dissipation (QCM-D) and high-energy X-ray reflectivity (XRR). Our experimental findings suggest that the lipid oxidation up to 20 mol % leads to the rupture of vesicles right after the adsorption. Our XRR analysis unravels the membrane thinning and the decrease in the lateral ordering of lipids, which can be explained by the decrease in the lateral packing of hydrocarbon chains. Further studies on mechanics of membranes incorporating oxidized lipids can be attributed to the decrease in the bending rigidity and the increase in the permeability.



INTRODUCTION

Cell membranes are one of the most important components of biological systems forming a protective barrier of living cells by separating the cytoskeleton from the external compartment. They are involved in several cellular functions and processes, such as cell protection, signaling, and communication of cells with each other and with their surrounding environments.¹ They consist of phospholipids with various headgroups and chains. However, the membranes of eukaryotic cells are composed of large amounts of diacylglycerophospholipids² with a high occurrence of polyunsaturated fatty acid (PUFA) chains³ that are subject to oxidative modification. The changes in the physical properties of biological membranes caused by the phospholipid oxidation,⁴ such as decrease in the lateral packing⁵ and thinning of the bilayer,⁶ are expected to cause several pathological and physiological consequences.^{7–11}

The glycerophospholipids of mammalian cells are composed of a saturated fatty acyl chain of either 16 or 18 carbons which is usually linked to the sn-1 position, while the sn-2 position is usually connected to a mono or polyunsaturated chain.^{3,12,13} Although polyunsaturated chains are abundant in few specialized organelles such as mitochondria,¹⁴ they can be also found in lipoprotein particles and cellular membranes which are considered as the major source for OxPLs generation.^{11,12,15} Indeed, among the PUFAs, docosahexaenoic acid (DHA) can be found at concentrations of several mol % in

membranes of most organs;¹⁶ however, the concentration becomes higher in the neural cells and networks such as in brain frontal cortex, retina, and mammalian synapsis, where the DHA concentration can reach 15 to 50 mol %.^{16,17}

Thus, most of the OxPLs are modified at the sn-2 position of the glycerol backbone to different types of truncated oxidized phospholipids depending on the acyl chain length and its degree of unsaturation.^{12,18} The oxidized acyl chains are thus shorter in length than the parent molecules and bear polar functional group (aldehydes or carboxylic group) at the chain terminus.¹² Among these oxidized phospholipids, PazePC and PoxnoPC are two stable lipid oxidation products originated from POPC oxidation. PazePC and PoxnoPC bear carboxyl and aldehyde groups at the end of truncated sn-2 chains. PoxnoPC is one of the key products of ozone mediated oxidation of lung surfactants and promotes apoptosis and necrosis.¹⁹ PazePC has been detected in LDL particles and has been implicated in the genesis of atherosclerosis.²⁰ At neutral pH, the aldehyde and carboxyl groups bear neutral and negative charges, respectively. In addition, recent molecular dynamics simulation study⁶ suggests that a large free-energy penalty to embed a charged carboxyl group of PazePC in the hydrophobic

Received: December 11, 2014

Revised: April 2, 2015

Published: April 14, 2015

core of a lipid bilayer induces the reorientation of the oxidized chain into the aqueous phase. Although several studies have demonstrated the presence of oxidized phospholipids in many pathological states, previous studies on the effect of oxidation of acyl chains at the *sn*-2 position on the structural integrity of membranes have been mostly performed on vesicle suspensions and monolayers at the air/water interface using the mixtures of OxPLs and matrix lipids in a molar fraction up to 20 mol %.^{21–23} To date, the concentration of oxidized phospholipids (OxPLs) in biological membranes has not been quantified. However, it should be noted that the expression level of OxPLs can be very high in some organelles such as mitochondria, since it is the main source of ROS as already pointed out by Volinsky et al.²³ and Chen et al.²⁴

The primary aim of this work is to investigate the impact of phospholipid oxidation on the formation process and the fine structures of supported planar bilayers by incorporating a defined amount of biologically relevant PazePC and PoxnoPC.^{25,26} To achieve this goal, we monitored the kinetics of formation of planar phospholipid membranes containing different molar fractions of OxPLs on solid substrates by using quartz crystal microbalance with dissipation monitoring (QCM-D). Indeed, it has been shown that QCM-D is an efficient tool to study the formation mechanism of SLBs^{27,28} by providing information about the mass of an adsorbed material and its viscoelastic properties. Moreover, X-ray reflectivity (XRR) measurements at high energy (17.48 keV) guarantee sufficiently high transmittance of X-ray beam through bulk water and thus enable one to study the impact of lipid oxidation on the membrane fine-structures at the solid/liquid interface, such as the thickness and density of hydrocarbon chains and head groups and roughness of each interface in the presence and absence of OxPLs.^{29,30} Therefore, the combination of QCM-D and XRR would provide a comprehensive view of the impact of OxPLs on the physicochemical properties of lipid bilayer.

MATERIALS AND METHODS

Chemicals. 1-Palmitoyl-2-oleoyl-*sn*-glycero-3-phosphocholine (POPC), 1-palmitoyl-2-(9'-oxo-nonanoyl)-*sn*-glycero-3-phosphocholine (PoxnoPC), and 1-palmitoyl-2-azelaoyl-*sn*-glycero-3-phosphocholine (PazePC) were provided from Avanti Polar Lipids (Alabaster, AL) and were used without further purification. HEPES buffer and NaCl were purchased from Sigma-Aldrich (Munich, Germany). In all experiments, ultrapure water (Millipore, Molsheim, France) with a resistivity of 18.2 M Ω cm was used.

Vesicles Preparation. The preparation of the Small Unilamellar Vesicles (SUV) of POPC, POPC-Paze PC, and POPC-Poxno PC (see Figure 1) was done by the hydration of the dry lipid film also known by Bangham's method,³¹ followed by the extrusion of vesicles suspensions.³² The desired amount of phospholipid mixture in chloroform/methanol (9:1 v/v) was added in a round flask, and the organic solvent was evaporated under reduced pressure for 3 h. Afterward, the HEPES buffer (10 mM, pH 7.4, NaCl 50 mM) was added at 40 °C to hydrate the resulting dry lipid film to get a final lipid concentration of 2 mM.³³ The lipid suspension thus obtained was then extruded at room temperature 15 times through 200 and 50 nm pore diameter polycarbonate membranes using a LiposoFast extruder (Avestin, Mannheim, Germany). For QCM-D and XRR experiments, the liposomes have been diluted just before measurements in HEPES buffer (10 mM, pH 7.4, NaCl 150

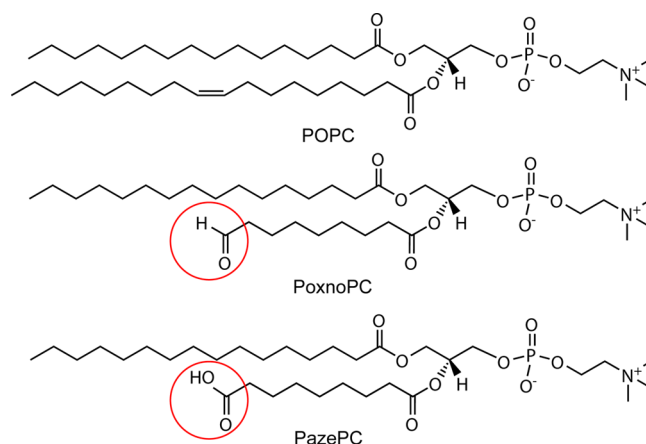


Figure 1. Chemical structures of 1-palmitoyl-2-oleoyl-*sn*-glycero-3-phosphocholine (POPC) and the two oxidatively modified phospholipids used in the present study: 1-palmitoyl-2-(9'-oxo-nonanoyl)-*sn*-glycero-3-phosphocholine (PoxnoPC) and 1-palmitoyl-2-azelaoyl-*sn*-glycero-3-phosphocholine (PazePC).

mM) to get a final concentration of lipids of 0.2 mM. A Zeta-sizer (Nano ZS, Malvern, U.K.) was used to measure the hydrodynamic diameter and zeta potential (ζ) of the vesicles after their dilution in deionized water to get a final concentration of NaCl of 5 mM. This low ionic strength was used to reduce the high conductivity of vesicle suspension during zeta potential measurements. All DLS measurements were carried out at 20 °C. The average hydrodynamic radius of liposomes was 50 nm for all formulations. It should be noted, that the dilution of liposome suspension with either deionized water or Hepes buffer (i.e., under isotonic conditions) did not induce any significant change in the PDI and size of the liposomes (Figure S1 of the Supporting Information).

Quartz Crystal with Dissipation Monitoring (QCM-D). The rupture kinetics of lipid vesicles was studied using a QCM-D E4 instrument from Q-Sense (Gothenburg, Sweden) equipped with four independent channels and a peristaltic pump. The silicon dioxide (SiO₂) coated quartz crystals (AT-cut, $f_0 = 5$ MHz) were supplied by Q-Sense AB. Prior to their use, the crystals were soaked in 10 mM sodium dodecyl sulfate (SDS) solution for 1 h, followed by rinsing with ultrapure water, dried under a N₂ stream, and treated in a UV-ozone chamber for 20 min.³³ SUV suspensions (2 mM in HEPES) were diluted in HEPES buffer (10 mM, NaCl 150 mM, pH 7.4) just before the experiment to get a final concentration of lipids of 0.2 mM and were then flowed on the SiO₂-coated quartz crystals for ~ 15 min until Δf and D signals were stable.³⁴ Afterward, the lipid bilayer was rinsed with HEPES buffer for ~ 10 min. The flow rate of the peristaltic pump was set to 100 μ L/min, and the temperature was stabilized at 25 ± 0.1 °C.

High Energy Specular X-ray Reflectivity (XRR). XRR curves were measured using a D8 Advance diffractometer (Bruker, Germany) operating with a sealed X-ray tube emitting Mo K α radiation ($E = 17.48$ keV, $\lambda = 0.0709$ nm). The beam size was defined to 200 μ m in the scattering plane after its collimation by various slits. To avoid the sample radiation damage, the attenuator was set to automatic. In approximately 3 h, the XRR scans were completed. Before the formation of supported planar bilayer, the cleaned Si wafers were placed into a Teflon chamber with Kapton windows. The momentum transfer normal to the plane of the membrane is given as a function of the angle of incidence α_i , $q_z = (4\pi/\lambda)\sin \alpha_i$.

With the aid of an in-beam monitor, the reflectivity for each measurement point was corrected for the beam footprint and for the beam intensity. A genetic minimization algorithm of the Parratt formalism³⁵ implemented in the Motofit software package³⁶ was used to fit the experimental data.

RESULTS AND DISCUSSION

Membrane Formation Monitored by QCM-D. In order to investigate the effect of OxPIs on the formation of planar phospholipid membranes, we monitored their kinetics of formation on solid substrates by using QCM-D (Table 1,

Table 1. Maximal Change in Resonant Frequency, Δf_{\max} , the Difference in Frequency, Δf_{mem} , and Energy Dissipation, ΔD , before and after the Membrane Formation Monitored by QCM-D^a

vesicle composition	Δf_{\max} (Hz)	Δf_{mem} (Hz)	ΔD_{mem} (10^{-6})
POPC	-43.2 ± 0.9	-26.1 ± 0.4	0.30 ± 0.27
PazePC 10%	-30.6 ± 0.2	-24.8 ± 1.3	0.30 ± 0.15
PazePC 20%	–	-24.0 ± 1.1	0.11 ± 0.12
PoxnoPC 10%	-39.2 ± 6.1	-26.2 ± 0.7	0.36 ± 0.14
PoxnoPC 20%	–	-24.8 ± 0.7	0.29 ± 0.04

^aEach reported value is the average \pm standard deviation of at least 3 different measurements.

Figure 2). Prior to the deposition onto solid substrates, POPC vesicles incorporating up to 20 mol % of PazePC or PoxnoPC were extruded to gain monodisperse, small unilamellar vesicles with a hydrodynamic radius of ~ 50 nm, which was confirmed by dynamic light scattering (Table 2). Figure 2A represents the change in Δf and ΔD during the formation of supported membrane for pure POPC vesicles monitored at 35 MHz ($n = 7$). Following the injection of POPC vesicles, an abrupt decrease in the frequency ($\Delta f_{\text{POPC}} = -43.2$ Hz) and a simultaneous increase in the dissipation ($\Delta D = 2.9 \times 10^{-6}$) was observed, suggesting the adsorption of intact lipid vesicles.²⁸ Then, a minimum in resonance frequency shift and a maximum in energy dissipation were obtained, indicating that a critical density of adsorbed vesicles was reached. At this point, the rupture of vesicles into planar membranes started and could be identified by an increase in Δf and a simultaneous decrease in ΔD due to the release of trapped water from the inner core of vesicles. Afterward, the saturation levels, $\Delta f_7 = -26.1$ Hz and $\Delta D = 0.3 \times 10^{-6}$ for POPC vesicles were reached, indicating the formation of a stable supported membrane.²⁸

The incorporation of OxPIs into POPC alters significantly the vesicle rupture process. Indeed, when working with POPC/Paze PC vesicles (at 10 mol %), the maximal change resonance frequency Δf_{\max} decreased significantly ($\Delta f_{\max} = -30.6$ Hz) compared to pure POPC (Figure 2B, Table 1). This result indicates that the onset of the bilayer formation occurs at lower surface coverage with vesicles. When the molar fraction of PazePC was increased to 20 mol % (Figure 2C), we observed no distinct minimum in Δf . Nevertheless, it should be noted that the resonant frequency values after the membrane formation Δf_{mem} were comparable in the presence and absence of PazePC ($\Delta f_{\text{mem}} \sim -25 \pm 1$ Hz). When PoxnoPC was incorporated into POPC membranes, we observed the same tendency, but the effect was less pronounced. $\Delta f_{\max} \sim -39.2$ Hz for the vesicles doped with 10 mol % PoxnoPC (Figure 2D, Table 1) suggests that the critical coverage for the vesicle rupture is in between those of pure POPC and POPC doped

with 10 mol % PazePC. Similar to PazePC, the formation of membranes containing 20 mol % of PoxnoPC did not exhibit a distinct minimum, where the vesicles ruptured in one step (Figure 2E). Moreover, the kinetics of membrane formation were found to be slower than that of PazePC (Figure 2C), suggesting that vesicles doped with PoxnoPC are more persistent to the rupture compared to PazePC-containing vesicles. The fact that vesicles containing high amount of OxPIs (20 mol %) immediately form planar bilayer membranes suggests that these vesicles rupture upon the contact to solid surface without reaching to the critical coverage level.

Spontaneous fusion of vesicles upon the contact to solid substrates has been reported for vesicles of positively charged phospholipids on SiO₂ substrates, which was interpreted in terms of the attractive electrostatic interactions.^{37,38} In case of zwitterionic or negatively charged phospholipids, the spontaneous vesicle fusion was demonstrated under high osmotic pressures or in the presence of divalent ions.^{38,39} However, our experimental finding can be attributed to neither the electrostatic attraction nor the ionic bridge via divalent cations: POPC, PazePC, and PoxnoPC do not carry positive charges, and the experiments were performed at the same osmotic pressure for all mixtures and without adding divalent ions into the buffer. In fact, molecular dynamics (MD) simulation by Khandelia et al.⁶ as well as the experimental study on monolayers²¹ suggested that the oxidized chain of PazePC is reoriented into the aqueous phase. This hypothesis was also confirmed by our zeta potential measurements, demonstrating that the zeta potentials of vesicles become more negative with the increase in PazePC fractions (Table 2). Regarding Poxno PC containing vesicles, their zeta potential remains almost unchanged compared to pure POPC liposomes. Such a result is consistent with the zwitterionic character of Poxno PC at neutral pH. The aforementioned result along with differential scanning calorimetry (DSC) measurements, showing distinct broadening and suppression of the main phase transition peaks according to the increase in the molar fraction of OxPI (Figure S2 of the Supporting Information). Although it is not possible to exclusively conclude if all OxPIs were incorporated into the membranes by DSC, this finding provides with supporting evidence that OxPIs were incorporated into matrix lipids as substitutional impurities that disturb chain ordering.

Thus, the spontaneous fusion of vesicles into planar membranes could rather be interpreted in terms of the mechanical instability of vesicles containing large fractions (20 mol %) of OxPIs. Henriksen et al.⁴⁰ recently proposed the mechanism of how the partition of detergents, such as lysolipids, would influence the mechanical properties of phospholipid vesicles by the combination of isothermal titration calorimetry (ITC) and the flicker spectroscopy.^{41,42} It has been demonstrated that the partition coefficient of detergents is inversely proportional to the critical micelle concentration, which depends on the length of hydrocarbon chains. Moreover, the mechanical perturbation (softening) also strongly depends on the length mismatch of hydrocarbon chains between detergents and matrix lipids. In our experimental systems, the lipid oxidization and thus the reorientation of oxidized carboxyl groups disturbs the ordering of hydrocarbon chains, leading to changes in the packing parameters,⁴³ which is defined by $P = (Al/V)$, where A , l , and V stand for the cross-sectional area of the headgroup, the axial length, and the volume of the molecules, respectively. Although the small unilamellar vesicles used for the vesicles fusion in our study may not significantly

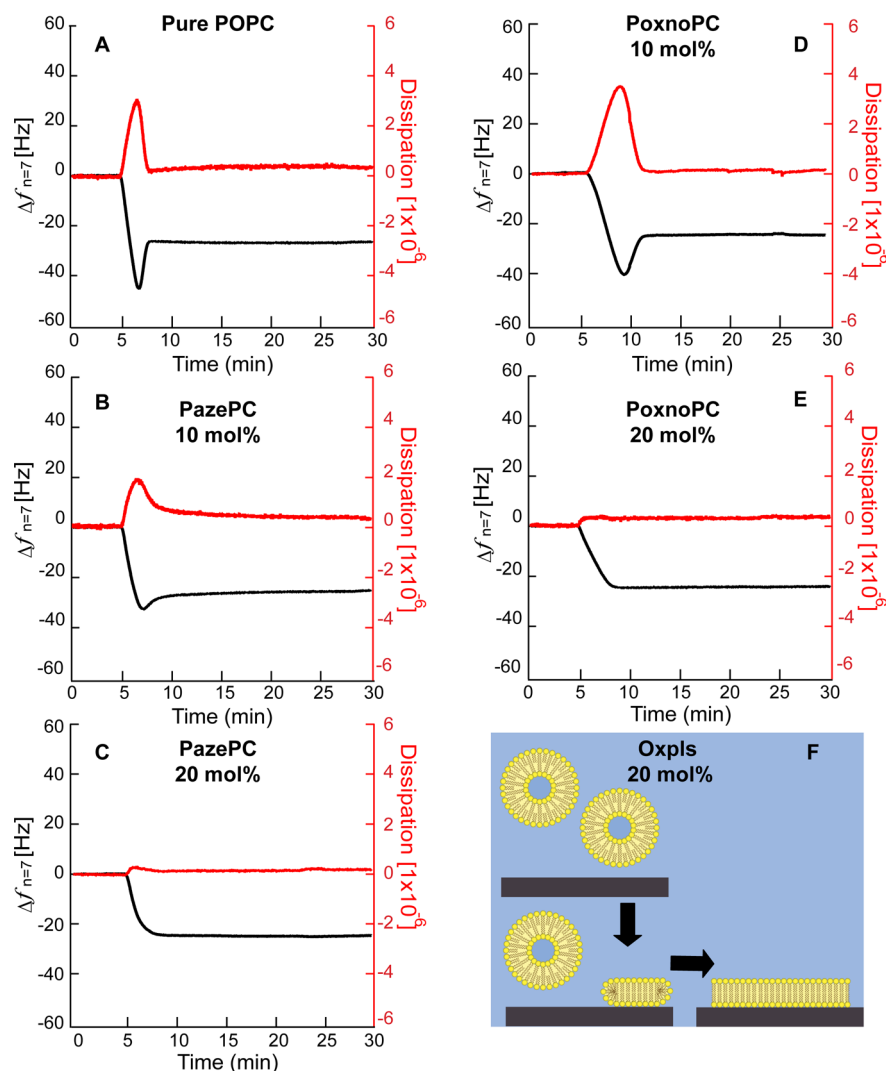


Figure 2. Changes in resonant frequency Δf (black) and dissipation ΔD (red) monitored at 35 MHz ($n = 7$) during formation of planar membranes on SiO_2 substrates in the (a) absence and (b and c) presence of PazePC and (d and e) PoxnoPC. (f) The obtained results suggest that the vesicles with 20 mol % OxPl are spread upon their contact to solid substrates without waiting for the accumulation of adsorbed vesicles.

Table 2. Hydrodynamic Radius (nm) and Zeta Potential (ζ) (mV) of Vesicles Suspension

composition	R (nm)	vesicles zeta potential (ζ) (mV)
POPC	49	-12.5 ± 3.5
PazePC 10%	51	-25.7 ± 1.9
PazePC 20%	46	-31.2 ± 1.4
PoxnoPC 10%	48	-11.7 ± 1.0
PoxnoPC 20%	47	-8.5 ± 1.0

depend on the curvature instability due to the penalty of bending energy by the extrusion, it is plausible that the packing strain caused by the presence of OxPls beyond a certain threshold mechanically destabilizes the vesicles, resulting in the spontaneous rupture upon the contact to substrates.

XRR. To get a better understanding on the effect of the OxPls on the fine-structures of supported membranes perpendicular to the global plane of membranes, the specular X-ray reflectivity (XRR) in the absence and presence of OxPls was measured at high energy (17.48 keV). Figure 3A shows the XRR curves of a pure POPC bilayer (black) and with 20 mol % of PazePC (red). The corresponding electron density profiles

reconstructed from the best fit results (black lines) were presented in Figure 3B. The reflectivity curves were best fitted using a 5-slab model, including outer head groups, alkyl chains, inner head groups, water reservoir, and SiO_2 . As previously reported, the reflectivity of pure POPC membranes (black) exhibit two pronounced minima, confirming POPC forms layered structures with clear electron density contrasts. The reflectivity curves (Figure 3A, red) and the reconstructed electron density profile (Figure 3B, red) suggest that the incorporation of 20 mol % PazePC leads to a shift in the positions of the first and second minima toward higher q values, implying that the lipid oxidation up to a level of 20 mol % results in a decrease in the total membrane thickness ($\Delta d = 2.8 \text{ \AA}$), which can be identified from the layer parameters, such as thickness d , electron density (ρ), and root-mean-square roughness (σ) summarized in Table 3. The slight decrease in the membrane thickness can be attributed to the packing strain caused by the reorientation of oxidized groups and thus disturbance to the chain order, which could be characterized by a slight increase in the electron density in the outer head groups and hydrocarbon chain regions. The membrane incorporating 20 mol % PoxnoPC qualitatively exhibited the same tendency

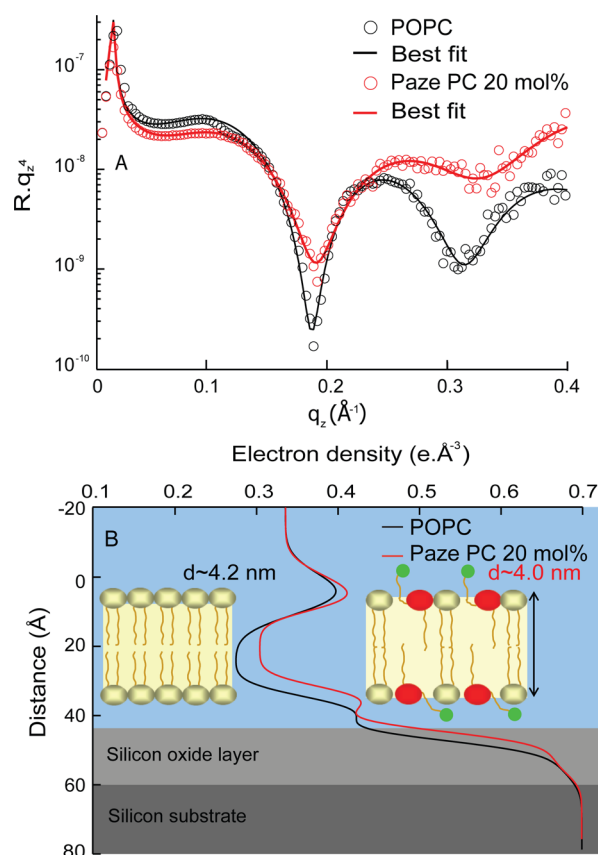


Figure 3. (A) XRR curves of a pure POPC supported membranes (black) and POPC-Paze PC 20 mol % (red). The solid lines represent the best model fits to the experimental data. The experimental errors are within the symbol size. (B) The corresponding electron density profiles of a pure POPC membrane (black) and POPC-Paze PC 20 mol % (red).

Table 3. Best Fit Parameters ($\chi^2 \leq 0.01$) for the XRR Results for Pure POPC Membrane and Incorporating 20 mol % of PazePC or PoxnoPC as Presented in Figures A and B

POPC	d (Å)	ρ ($e \times \text{Å}^{-3}$)	σ (Å)
outer headgroup	10.0	0.436	5.2
alkyl chains	24.1	0.287	4.7
inner headgroup	8.1	0.454	3.4
water	3.9	0.335	3.2
SiO ₂	10.5	0.660	3.3
20 mol % Paze PC	d (Å)	ρ ($e \times \text{Å}^{-3}$)	σ (Å)
outer headgroup	8.5	0.440	5.0
alkyl chains	22.8	0.301	3.3
inner headgroup	8.1	0.447	3.4
water	4.1	0.335	3.2
SiO ₂	12.3	0.660	3.2
20 mol % Poxno PC	d (Å)	ρ ($e \times \text{Å}^{-3}$)	σ (Å)
outer headgroup	9.9	0.443	5.0
alkyl chains	22.7	0.305	4.6
inner headgroup	8.0	0.454	3.3
water	3.8	0.335	3.2
SiO ₂	12.8	0.660	3.1

(Figure 4, blue). However, the decrease in the total thickness was less pronounced compared to the effect caused by the incorporation of 20 mol % PazePC.

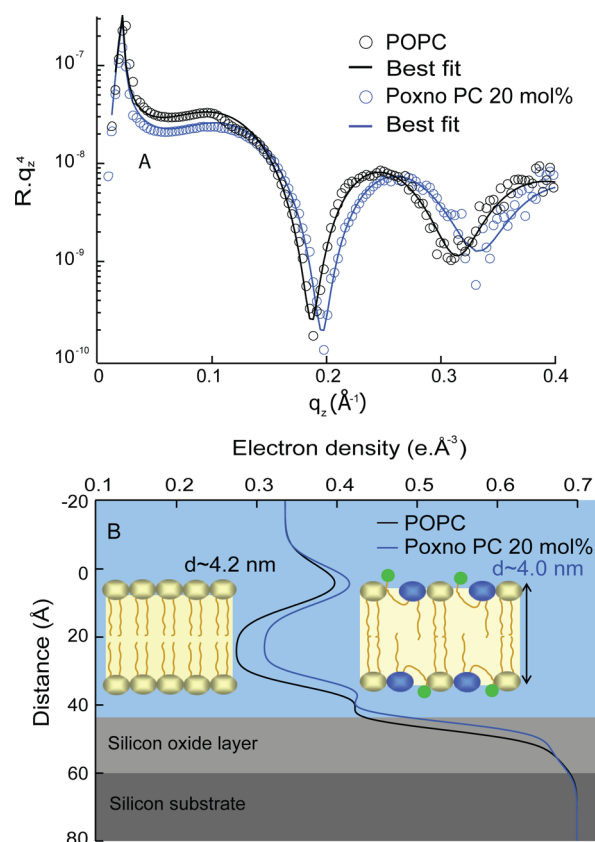


Figure 4. (A) XRR curves of a pure POPC supported membranes (black) and POPC-Poxno PC 20 mol % (blue). The solid lines represent the best model fits to the experimental data. The experimental errors are within the symbol size. (B) The corresponding electron density profiles of a pure POPC membrane (black) and POPC-Poxno PC 20 mol % (blue).

The reorientation of the oxidized moieties and thus the disordering of the chain packing could lead to the creation of free voids where water molecules could permeate into deeper inside of the membrane core. In fact, previous experimental studies demonstrated that the illumination with UV light and sunlight^{44,45} as well as γ -ray⁴⁶ results in a clear increase in the permeability of water and glucose across liposomal membranes. More recently, Lis et al. combined stopped-flow experiments and MD simulations and demonstrated that the free-energy barrier of water was significantly reduced in the presence of oxidized phospholipids.²² In addition, Volinsky et al.²³ have performed dithionite-based quenching assays, demonstrating that the addition of dithionite to POPC vesicles with Paze PC or Poxno PC content ≥ 20 mol % resulted in an immediate and complete quenching of the transbilayer NBD fluorophore.²³

Nevertheless, our fine-structure analysis clearly indicated that the presence of OxPIs did not cause any remarkable increase in the interfacial roughness, indicating thus that the overall integrity of the stratified membrane structure was preserved even in the presence of 20 mol % of OxPIs. Our experimental results have demonstrated for the first time that the lipid oxidization to the level of 20 mol % leads to the thinning of phospholipid membranes and thus the decrease in the packing order of lipid molecules without destroying their layer-by-layer structures, which is in good agreement with the change in electron density profiles predicted by MD simulations.⁶

The changes in membrane fine-structures, such as decrease in the thickness and the disordering of hydrocarbon chains, are expected to influence the mechanical properties of membranes. For example, the decrease in the membrane thickness and the increase in the permeability against solutes would lead to a decrease in the bending stiffness, which would result in the energetic barrier for the rupture of vesicles upon the contact to solid substrates.⁴⁷

SUMMARY AND CONCLUSIONS

We physically modeled the effect of lipid oxidization on the physicochemical properties of model biomembranes in a quantitative manner. As defined membrane models, we fabricated supported membranes in the absence and presence of two different OxPLs, PazePC with a carboxyl group and PoxnoPC with an aldehyde group. The kinetics of membrane formation on solid substrates was monitored using QCM-D. It is noteworthy that pure POPC membranes and membranes incorporating 10 mol % of OxPLs follows the classical pathway, where the rupture of vesicles occurs after reaching a critical density of vesicles on substrates. In contrast, once the level of lipid oxidization reaches 20 mol %, vesicles undergo simultaneous rupturing upon their contact to substrates, irrespective of the electrostatic interactions between vesicles and the underlying substrates. The fine structures of membranes in the presence and absence of OxPL were analyzed with high-energy XRR, quantitatively demonstrating that the incorporation of 20 mol % of PazePC and PoxnoPC induce a decrease in the membrane thickness accompanied by an increase in the electron density of hydrocarbon chains, suggesting an increase in membrane permeability while sustaining the structural integrity of membranes. The obtained results suggest that the reorientation of oxidized moieties should decrease in both the membrane thickness and the lateral packing of hydrocarbon chains, which may result in the permeability and in the decrease of the bending rigidity. Therefore, it has been concluded that the mechanically destabilized vesicles may undergo the simultaneous rupture on solid substrates. It has been demonstrated that the combination of QCM-D and XRR is a powerful tool providing with the mechanistic insights into the effect of level of lipid oxidization on the physicochemical properties of cell membranes.

ASSOCIATED CONTENT

Supporting Information

DLS measurements of POPC-Paze PC 20 mol % liposomes diluted either in deionized water or HEPES buffer (1), DSC measurements of SOPC liposomes doped with OxPLs (2). This material is available free of charge via the Internet at <http://pubs.acs.org>.

AUTHOR INFORMATION

Corresponding Author

*E-mail: tanaka@uni-heidelberg.de.

Present Address

^{||}(A.M.) CNRS UMR 8612, Institut Galien Paris-Sud, Faculté de Pharmacie, 5 rue J.B. Clément, 92296 Châtenay-Malabry, France.

Notes

The authors declare no competing financial interest.

ACKNOWLEDGMENTS

We thank A. Burk, N. Frenkel, and W. Abuillan for helpful discussion on XRR experiments and N. Ibrahim for proof-reading this manuscript. This work was supported by Phospholipid Research Center and JSPS/MEXT KAKENHI (Grants 26247070 and 26103521). A.M. is thankful to the Alexander von Humboldt Foundation for the postdoctoral fellowship. M.T. is a member of German Excellence Cluster "Cell Networks" and Helmholtz Program BioInterfaces. iCeMS is supported by World Premier International Research Center Initiative (WPI), MEXT, Japan.

REFERENCES

- (1) Sackmann, E. *Biological Membranes Architecture and Function*. In *Handbook of Biological Physics*, Lipowsky, R.; Sackmann, E., Eds.; North-Holland Publishing Company: Amsterdam, 1995; Vol. 1, pp 1–63.
- (2) Hauser, H.; Poupart, G. *Lipid Structure*. In *The Structure of Biological Membranes*, 2nd ed.; Yeagle, P. L., Ed. CRC Press: Boca Raton, FL, 2004; pp 1–49.
- (3) Hulbert, A. J.; Rana, T.; Couture, P. The Acyl Composition of Mammalian Phospholipids: an Allometric Analysis. *Comp. Biochem. Physiol., Part B: Biochem. Mol. Biol.* **2002**, *132*, 515–527.
- (4) Jurkiewicz, P.; Olzyska, A.; Cwiklik, L.; Conte, E.; Jungwirth, P.; Megli, F. M.; Hof, M. Biophysics of Lipid Bilayers Containing Oxidatively Modified Phospholipids: Insights from Fluorescence and EPR Experiments and from MD Simulations. *Biochim. Biophys. Acta, Biomembr.* **2012**, *1818*, 2388–2402.
- (5) Wratten, M. L.; van Ginkel, G.; van't Veld, A. A.; Bekker, A.; van Faassen, E. E.; Sevanian, A. Structural and Dynamic Effects of Oxidatively Modified Phospholipids in Unsaturated Lipid Membranes. *Biochemistry* **1992**, *31*, 10901–10907.
- (6) Khandelia, H.; Mouritsen, O. G. Lipid Gymnastics: Evidence of Complete Acyl Chain Reversal in Oxidized Phospholipids from Molecular Simulations. *Biophys. J.* **2009**, *96*, 2734–2743.
- (7) Catala, A. Lipid Peroxidation of Membrane Phospholipids generates Hydroxy-alkenals and Oxidized Phospholipids Active in Physiological and/or Pathological Conditions. *Chem. Phys. Lipids* **2009**, *157*, 1–11.
- (8) Markesbery, W. R. Oxidative Stress Hypothesis in Alzheimer's Disease. *Free Radical Biol. Med.* **1997**, *23*, 134–147.
- (9) Berliner, J. A.; Leitinger, N.; Tsimikas, S. The Role of Oxidized Phospholipids in Atherosclerosis. *J. Lipid Res.* **2009**, *50* (Suppl), 207–212.
- (10) Yoshimi, N.; Ikura, Y.; Sugama, Y.; Kayo, S.; Ohsawa, M.; Yamamoto, S.; Inoue, Y.; Hirata, K.; Itabe, H.; Yoshikawa, J.; et al. Oxidized Phosphatidylcholine in Alveolar Macrophages in Idiopathic Interstitial Pneumonias. *Lung* **2005**, *183*, 109–121.
- (11) Bochkov, V. N. Inflammatory Profile of Oxidized Phospholipids. *Thromb. Haemostasis* **2007**, *97*, 348–354.
- (12) Fruhwirth, G. O.; Loidl, A.; Hermetter, A. Oxidized Phospholipids: from Molecular Properties to Disease. *Biochim. Biophys. Acta, Mol. Basis Dis.* **2007**, *1772*, 718–736.
- (13) Mohammad, Z. A.; Swati, S. Oxidized Phospholipids: Introduction and Biological Significance. In *Lipoproteins: Role in Health and Diseases*; Frank, S.; Kostner, G., Eds.; InTech: Rijeka, Croatia, 2012; pp 409–430.
- (14) Pepe, S. Effect of Dietary Polyunsaturated Fatty Acids on Age-Related Changes in Cardiac Mitochondrial Membranes. *Exp. Gerontol.* **2005**, *40*, 751–758.
- (15) Bochkov, V. N.; Oskolkova, O. V.; Birukov, K. G.; Levonen, A. L.; Binder, C. J.; Stockl, J. Generation and Biological Activities of Oxidized Phospholipids. *Antioxid. Redox Signaling* **2010**, *12*, 1009–1059.
- (16) Klaus, G. The Dynamics of Membrane Lipids. In *The Structure of Biological Membranes*, 2nd ed.; Yeagle, P. L., Ed. CRC Press: Boca Raton, 2004; pp 147–167.

- (17) Moriguchi, T.; Salem, N., Jr. Recovery of Brain Docosahexaenoate leads to Recovery of Spatial Task Performance. *J. Neurochem.* **2003**, *87*, 297–309.
- (18) Deigner, H. P.; Hermetter, A. Oxidized Phospholipids: Emerging Lipid Mediators in Pathophysiology. *Curr. Opin. Lipidol.* **2008**, *19*, 289–294.
- (19) Uhlson, C.; Harrison, K.; Allen, C. B.; Ahmad, S.; White, C. W.; Murphy, R. C. Oxidized Phospholipids Derived from Ozone-treated Lung Surfactant Extract reduce Macrophage and Epithelial Cell Viability. *Chem. Res. Toxicol.* **2002**, *15*, 896–906.
- (20) Davies, S. S.; Pontsler, A. V.; Marathe, G. K.; Harrison, K. A.; Murphy, R. C.; Hinshaw, J. C.; Prestwich, G. D.; Hilaire, A. S.; Prescott, S. M.; Zimmerman, G. A.; et al. Oxidized Alkyl Phospholipids are Specific, High Affinity Peroxisome Proliferator-Activated Receptor Gamma Ligands and Agonists. *J. Biol. Chem.* **2001**, *276*, 16015–16023.
- (21) Sabatini, K.; Mattila, J. P.; Megli, F. M.; Kinnunen, P. K. Characterization of Two Oxidatively Modified Phospholipids in Mixed Monolayers with DPPC. *Biophys. J.* **2006**, *90*, 4488–4499.
- (22) Lis, M.; Wizert, A.; Przybylo, M.; Langner, M.; Swiatek, J.; Jungwirth, P.; Cwiklik, L. The Effect of Lipid Oxidation on The Water Permeability of Phospholipids Bilayers. *Phys. Chem. Chem. Phys.* **2011**, *13*, 17555–17563.
- (23) Volinsky, R.; Cwiklik, L.; Jurkiewicz, P.; Hof, M.; Jungwirth, P.; Kinnunen, P. K. Oxidized Phosphatidylcholines Facilitate Phospholipid Flip-Flop in Liposomes. *Biophys. J.* **2011**, *101*, 1376–1384.
- (24) Chen, R.; Yang, L.; McIntyre, T. M. Cytotoxic Phospholipid Oxidation Products. Cell Death from Mitochondrial Damage and The Intrinsic Caspase Cascade. *J. Biol. Chem.* **2007**, *282*, 24842–24850.
- (25) Sackmann, E. Supported Membranes: Scientific and Practical Applications. *Science* **1996**, *271*, 43–48.
- (26) Tanaka, M.; Sackmann, E. Polymer-Supported Membranes as Models of The Cell Surface. *Nature* **2005**, *437*, 656–663.
- (27) Keller, C. A.; Kasemo, B. Surface Specific Kinetics of Lipid Vesicle Adsorption Measured with a Quartz Crystal Microbalance. *Biophys. J.* **1998**, *75*, 1397–1402.
- (28) Keller, C. A.; Glasmästar, K.; Zhdanov, V. P.; Kasemo, B. Formation of Supported Membranes from Vesicles. *Phys. Rev. Lett.* **2000**, *84*, 5443–5446.
- (29) Abuillan, W.; Schneck, E.; Körner, A.; Brandenburg, K.; Gutschmann, T.; Gill, T.; Vorobiev, A.; Konovalov, O.; Tanaka, M. Physical Interactions of Fish Protamine and Antisepsis Peptide Drugs with Bacterial Membranes Revealed by Combination of Specular X-ray Reflectivity and Grazing-Incidence X-ray Fluorescence. *Phys. Rev. E* **2013**, *88*, 012705.
- (30) Korner, A.; Abuillan, W.; Deichmann, C.; Rossetti, F. F.; Kohler, A.; Konovalov, O. V.; Wedlich, D.; Tanaka, M. Quantitative Determination of Lateral Concentration and Depth Profile of Histidine-Tagged Recombinant Proteins Probed by Grazing Incidence X-ray Fluorescence. *J. Phys. Chem. B* **2013**, *117*, 5002–5008.
- (31) Bangham, A. D.; Standish, M. M.; Watkins, J. C. Diffusion of Univalent Ions Across The Lamellae of Swollen Phospholipids. *J. Mol. Biol.* **1965**, *13*, 238–252.
- (32) Hope, M. J.; Bally, M. B.; Webb, G.; Cullis, P. R. Production of Large Unilamellar Vesicles by a Rapid Extrusion Procedure. Characterization of Size Distribution, Trapped Volume and Ability to maintain a Membrane Potential. *Biochim. Biophys. Acta, Biomembr.* **1985**, *812*, 55–65.
- (33) Makky, A.; Michel, J. P.; Maillard, P.; Rosilio, V. Biomimetic Liposomes and Planar Supported Bilayers for The Assessment of Glycodendrimeric Porphyrins Interaction with an Immobilized Lectin. *Biochim. Biophys. Acta, Biomembr.* **2011**, *1808*, 656–666.
- (34) Frenkel, N.; Makky, A.; Sudji, I. R.; Wink, M.; Tanaka, M. Mechanistic Investigation of Interactions between Steroidal Saponin Digitonin and Cell Membrane Models. *J. Phys. Chem. B* **2014**, *118*, 14632–14639.
- (35) Parratt, L. G. Surface Studies of Solids by Total Reflection of X-Rays. *Phys. Rev.* **1954**, *95*, 359–369.
- (36) Nelson, A. Co-Refinement of Multiple-Contrast Neutron/X-ray Reflectivity Data Using MOTOFIT. *J. Appl. Crystallogr.* **2006**, *39*, 273–276.
- (37) Richter, R.; Mukhopadhyay, A.; Brisson, A. Pathways of Lipid Vesicle Deposition on Solid Surfaces: A Combined QCM-D and AFM Study. *Biophys. J.* **2003**, *85*, 3035–3047.
- (38) Cho, N. J.; Frank, C. W.; Kasemo, B.; Hook, F. Quartz Crystal Microbalance with Dissipation Monitoring of Supported Lipid Bilayers on Various Substrates. *Nat. Protoc.* **2010**, *5*, 1096–10106.
- (39) Rossetti, F. F.; Textor, M.; Reviakine, I. Asymmetric Distribution of Phosphatidyl Serine in Supported Phospholipid Bilayers on Titanium Dioxide. *Langmuir* **2006**, *22*, 3467–3473.
- (40) Henriksen, J. R.; Andresen, T. L.; Feldborg, L. N.; Duelund, L.; Ipsen, J. H. Understanding Detergent Effects on Lipid Membranes: A Model Study of Lysolipids. *Biophys. J.* **2010**, *98*, 2199–205.
- (41) Brochard, F.; Lennon, J. F. Frequency Spectrum of The Flicker Phenomenon in Erythrocytes. *J. Phys. (Paris)* **1975**, *36*, 1035–1047.
- (42) Duwe, H. P.; Kaes, J.; Sackmann, E. Bending Elastic Moduli of Lipid Bilayers: Modulation by Solutes. *J. Phys. (Paris)* **1990**, *51*, 945–962.
- (43) Israelachvili, J. N.; Mitchell, D. J.; Ninham, B. W. Theory of Self-Assembly of Hydrocarbon Amphiphiles into Micelles and Bilayers. *J. Chem. Soc., Faraday Trans. 2* **1976**, *72*, 1525–1568.
- (44) Mandal, T. K.; Chatterjee, S. N. Ultraviolet- and Sunlight-Induced Lipid Peroxidation in Liposomal Membrane. *Radiat. Res.* **1980**, *83*, 290–302.
- (45) Chatterjee, S. N.; Agarwal, S. Liposomes as Membrane Model for Study of Lipid Peroxidation. *Free Radical Biol. Med.* **1988**, *4*, 51–72.
- (46) Nakazawa, T.; Nagatsuka, S. Radiation-Induced Lipid Peroxidation and Membrane Permeability in Liposomes. *Int. J. Radiat. Biol.* **1980**, *38*, 537–544.
- (47) Reimhult, E.; Hook, F.; Kasemo, B. Intact Vesicle Adsorption and Supported Biomembrane Formation from Vesicles in Solution: Influence of Surface Chemistry, Vesicle Size, Temperature, and Osmotic Pressure. *Langmuir* **2003**, *19*, 1681–1691.